Quasielastic Neutron Scattering Study of Hydrogen Motions in an Aqueous Poly(vinyl methyl ether) Solution

S. Capponi,[1,2,a)] A. Arbe,[3] S. Cerveny,[3] R. Busselez,[1] B. Frick,[4] J. P. Embs,[5] and J. Colmenero[1,2,3]

[1]*Donostia International Physics Center, Paseo Manuel de Lardizabal 4, 20018 San Sebastián, Spain*
[2]*Departamento de Física de Materiales UPV/EHU, Apartado 1072, 20080 San Sebastián, Spain*
[3]*Centro de Física de Materiales (CSIC, UPV/EHU) and Materials Physics Center MPC, Paseo Manuel de Lardizabal 5, E-20018 San Sebastián, Spain*
[4]*Institut Laue–Langevin, BP 156, 38042 Grenoble Cedex 9, France*
[5]*Laboratory for Neutron Scattering, ETH Zurich and PSI, CH-5232 Villigen PSI, Switzerland*

(Received 18 February 2011; accepted 28 April 2011; published online XX XX XXXX)

We present a quasielastic neutron scattering (QENS) investigation of the component dynamics in an aqueous Poly(vinyl methyl ether) (PVME) solution (30% water content in weight). In the glassy state, an important shift in the Boson peak of PVME is found upon hydration. At higher temperatures, the diffusive-like motions of the components take place with very different characteristic times, revealing a strong dynamic asymmetry that increases with decreasing T. For both components, we observe stretching of the scattering functions with respect to those in the bulk and non-Gaussian behavior in the whole momentum transfer range investigated. To explain these observations we invoke a distribution of mobilities for both components, probably originated from structural heterogeneities. The diffusive-like motion of PVME in solution takes place faster and apparently in a more continuous way than in bulk. We find that the T-dependence of the characteristic relaxation time of water changes at $T \lesssim 225$ K, near the temperature where a crossover from a low temperature Arrhenius to a high temperature cooperative behavior has been observed by broadband dielectric spectroscopy (BDS) [S. Cerveny, J. Colmenero and A. Alegría, Macromolecules, **38**, 7056 (2005)]. This observation might be a signature of the onset of confined dynamics of water due to the freezing of the PVME dynamics, that has been selectively followed by these QENS experiments. On the other hand, revisiting the BDS results on this system we could identify an additional "fast" process that can be attributed to water motions coupled with PVME local relaxations that could strongly affect the QENS results. Both kinds of interpretations, confinement effects due to the increasing dynamic asymmetry and influence of localized motions, could provide alternative scenarios to the invoked "strong-to-fragile" transition. © *2011 American Institute of Physics*. [doi:10.1063/1.3592560]

I. INTRODUCTION

The dynamical behavior of interfacial and confined water at super-cooled temperatures is a hot topic of research essentially because the properties of biopolymers (proteins and DNA) depend on the dynamics of water in the first hydration shell.[1–3] In this context liquid-water mixtures or water confined in nano-cavities are ideal systems for studying hydration water at low temperatures because crystallization can be avoided even below the homogeneous nucleation temperature (235 K). In addition, the dynamic behavior of super-cooled water is very controversially discussed in the literature. One of the questions is the existence of the so-called "strong-to-fragile" transition. Such transition is postulated because the characteristic times deduced from neutron scattering experiments show a very prominent change in their thermal dependence from high temperature super-Arrhenius to low temperature Arrhenius behavior in the region between 215 and 228 K.[4–9] This observation was interpreted as a fragile-to-strong transition from the high density (HDL) to the less fluid low density phase (LDL) of super-cooled water. However, by using broadband dielectric spectroscopy (BDS) such behavior was not observed for protein hydration water[10] or water confined in MCM-41.[6] Based on these BDS results, the neutron scattering phenomenology was explained invoking a split of two relaxations from the main structural relaxation at the same temperature as the proposed strong to fragile transition.[6,10]

The dielectric response of aqueous binary mixtures typically reveals a water relaxation process at low temperature.[11–15] At high water concentration (roughly $c_w \geq 30\,wt\%$), the temperature dependence of the relaxation time shows a crossover from a high-temperature non-Arrhenius behavior to low temperature Arrhenius in the temperature range where the system shows a glass transition process (T_g). In previous works,[15] we have associated this crossover at T_g with the appearance of finite size effects on water dynamics due to the freezing of the matrix where water molecules are apparently confined. In addition, the low temperature Arrhenius behavior seems to show some universal characteristics independently of the solute used in the mixing: the activation energy is $(0.54 \pm 0.02$ eV) and the shape of the response is symmetric.[15]

a)Author to whom correspondence should be addressed. Electronic mail: saracapp@gmail.com.

Exploiting the complementarity of different experimental techniques can certainly shed some light on this kind of problems. In particular, the combination of BDS and quasielastic neutron scattering (QENS) has proved to be essential to unravel different dynamical aspects of glass-forming systems, in particular of polymers.[16–19] While BDS covers a huge dynamic window, QENS provides spatial information and opens the possibility of selective studies in the system by deuterium labeling. This opportunity is of utmost interest for the investigation of multicomponent systems,[20] and in particular in aqueous solutions where the information provided by BDS is usually limited to the water component due to the overwhelming dielectric signal of water dipoles.

As mentioned above, most studies of dynamics in concentrated aqueous solutions have been focused on hydrated proteins.[4,11,21,22] Typical biological water environments (for instance in proteins) include hydrophilic and hydrophobic sites/regions/interactions. This dual character determines several properties such as the tertiary and quaternary structure of the protein and even more important folding properties could be governed by these interactions. In this work, we rather address the dynamics of an aqueous polymer solution because synthetic polymers are less complex than proteins. Water-polymer interactions and their mutual effects on the dynamics are issues of fundamental interest per se, but, in addition, their investigation could also shed some light on the problems involving biological samples. In this work, we have namely investigated a mixture of Poly(vinyl methyl ether) (PVME) and water ($c_w = 30\%$). Like proteins, PVME contains both hydrophilic and hydrophobic groups to interact with water. Therefore, water environment in solutions of PVME could resemble, at least in a naïve way, the water environment of a much complex protein, and we could expect that some general aspects of the influence of water on the local dynamics of the macromolecules could be extensible to biological systems.

The structural characterization of the PVME/water mixture by x-ray diffraction is first presented to address the changes in the structure factor upon hydration. The main focus of the paper is on the use of QENS techniques and isotopic labeling, that have allowed us to characterize the dynamical behavior of both components. On one hand, QENS on a sample hydrated with heavy water has revealed the hydrogen dynamics of PVME in solution. In addition to the motions in the supercooled liquid state, we have addressed the question how the vibrational density of states of PVME hydrogens is affected by the presence of water deep in the glassy state. On the other hand, QENS measurements on a fully hydrogenated sample (combined with the information obtained on the partially deuterated system) have allowed the characterization of the hydrogen motions in the water component. Both components present unusual stretching and non-Gaussian effects in their intermediate scattering functions, features that are also reported for biological systems. Calorimetric and BDS studies on the PVME/water solution were already published by some of us.[23] Here we have revisited those BDS results, which at very low temperature reveal a process that was not reported in the previous paper[23] and that, as we will show, could strongly affect the QENS results of the water component. The outcome of both, BDS and QENS, are considered in a common discussion and a possible scenario is proposed for the dynamics of both components in the solution. In addition to H-bond formation, structural heterogeneities and dynamic asymmetry seem to play crucial roles in the development of the peculiar phenomenology displayed by this mixture and also shared with biological systems. In addition, striking similarities with the behavior of polymer blends are found, highlighting the importance of dynamic asymmetry in all these binary mixtures.

II. EXPERIMENTAL

A. Samples

Poly(vinyl methyl ether) (PVME, chemical formula [-CH_2-CHO(CH_3)-]$_n$) with average molecular weight M_w of 21.9 Kg/mol was supplied by Sigma-Aldrich in aqueous solution (50 wt%). Dehydrated samples were first obtained by extensively drying the as received sample in a vacuum oven at 380 K. Complete removal of water was assured by FTIR measurements. Rehydrating the dry samples with H_2O or D_2O respectively during one week solutions with water concentration of 30 wt% (H_2O) and 32 wt% (D_2O) were obtained. With these concentrations, determined by sample weighting, the number of water molecules per monomer is equal to ≈ 1.4 for both samples.

A differential scanning calorimeter (DSC) TA Instrument Q2000 was used in standard mode to monitor both, the crystallization of the samples as well as the glass transition temperature. All the samples were sealed in hermetic aluminum pans and a cooling-heating cycle between T_g-100 K and T_g+30 K, at a rate of 10 K/min, was performed using helium as transfer gas with a flow rate of 25 ml/min; the annealing time between cooling and heating runs was 2 min. From the heat flow curves, T_g values were calculated as the onset point. The glass transition temperatures were found to be $T_g^{PVME} = 247$ K, $T_g^{PVME/D_2O} = 211$ K and $T_g^{PVME/H_2O} = 208$ K. In addition no crystallization on cooling was observed for the water containing samples.

For the neutron scattering experiments flat aluminum holders were used and the sample thicknesses were chosen to provide a transmission of about 90%, thus allowing multiple scattering effects to be neglected.

B. Dielectric spectroscopy

A broadband dielectric spectrometer, Novocontrol Alpha-N, was used to measure the complex dielectric permittivity $\epsilon^*(\omega) = \epsilon'(\omega) - i\epsilon''(\omega)$ $(\omega = 2\pi f)$ in the frequency range $10^{-2} - 10^6\,Hz$. The isothermal frequency scans were performed every 5 degrees over the temperature range $120 - 250\,K$. The sample temperature was controlled with a stability better than $\pm 0.1\,K$. The same samples were also measured in a higher frequency range $(10^6 - 10^9\,Hz)$ by using an Agilent rf impedance analyzer $4192B$. For both measurements parallel gold plated electrodes, with a diameter of 20 mm for the Alpha-N and of 10 mm for the high frequency range, were used, whereas the sample thickness was typically 0.1 mm.

Finally, to expand the frequency range up to $10\,GHz$, measurements at room temperature were made in the frequency range of $50\,MHz$ $10\,GHz$ using an integrated system of HP8361A vector network analyzer (VNA) and a dielectric probe kit HP85070E. The sample thickness was 2 cm.

C. Quasielastic neutron scattering

In a neutron scattering experiment, the intensity is measured as a function of energy transfer ($\hbar\omega$) and momentum transfer (Q). $Q = 4\pi sin(\theta/2)/\lambda$ is determined by the scattering angle θ and the wavelength of the incoming neutrons λ. The measured intensity contains incoherent and coherent contributions that are weighted according to the corresponding cross sections of the nuclei (σ_{inc}, σ_{coh}). Due to the large value of σ_{inc} for hydrogens the neutron intensity scattered by a protonated sample is dominated by the incoherent contribution of these atoms, revealing thus directly their incoherent scattering function, $S^H_{inc}(Q,\omega)$. The Fourier transforms of $S^H_{inc}(Q,\omega)$ are the intermediate incoherent scattering function $S^H_{inc}(Q,t)$ and the self part of the Van Hove correlation function $G^H_{self}(r,t)$. $G^H_{self}(r,t)$ is the probability of a given hydrogen to be at distance r from the position where it was located at a time t before. Incoherent scattering looks at correlations between the positions of the same nucleus at different times. Since deuterons show a much smaller cross-section than protons, selective deuteration allows a strong reduction of the contribution of a given component of the system to the scattered intensity. We have exploited this labeling technique to isolate the component dynamics in the PVME solution. In the sample with deuterated water PVME/D_2O the intensity scattered by the water component is mainly coherent and very weak. Diffraction measurements with polarization analysis on this sample show that the ratio between the coherent contribution and the total intensity in the maximum of the static structure factor ($Q \approx 1.5$Å^{-1}, see Fig. 1(b)) is about 17%.[24] Thus, the signal of PVME/D_2O in this Q-range is strongly dominated by the incoherent scattering function of the hydrogens in wet PVME. On the other hand, the intensity scattered by PVME/H_2O is basically of incoherent origin ($\sigma_{inc}/\sigma_{tot} = 0.94$), and contains both contributions, that of wet-PVME hydrogens and that from confined water hydrogens. Their relative weights are $\sigma_{inc}^{PVME}/\sigma_{inc}^{PVME/H_2O} = 0.69$, $\sigma_{inc}^{H_2O}/\sigma_{inc}^{PVME/H_2O} = 0.31$.

1. Time of flight

In the microscopic time region ($\approx 0.2 - 20$ ps), the self motions of PVME protons in the dry and wet samples (PVME and PVME/D_2O) were investigated by time-of-flight (ToF) techniques at 100 K. We used the spectrometer FOCUS at the spallation source SINQ (Paul Scherrer Institut, Villigen). With $\lambda = 5$Å, the energy resolution of the experiment was δE(HWHM)$\approx 45\mu$eV. Background corrections were performed by subtracting the intensity scattered by the empty cell and taking self-absorption into account. The detector efficiency was corrected by the measurement of a standard Vanadium sample that was also used as resolution. Measuring times of the order of 5 h were employed. The elastic intensity measured at 20 K provided the low-T-reference to normalize the data. The normalization was done such that the integrated areas of the spectra at 20 K corresponded to the total scattering cross-section per PVME monomer in each sample. The constant-Q spectra were obtained from interpolation of the data measured as function of constant scattering angle.

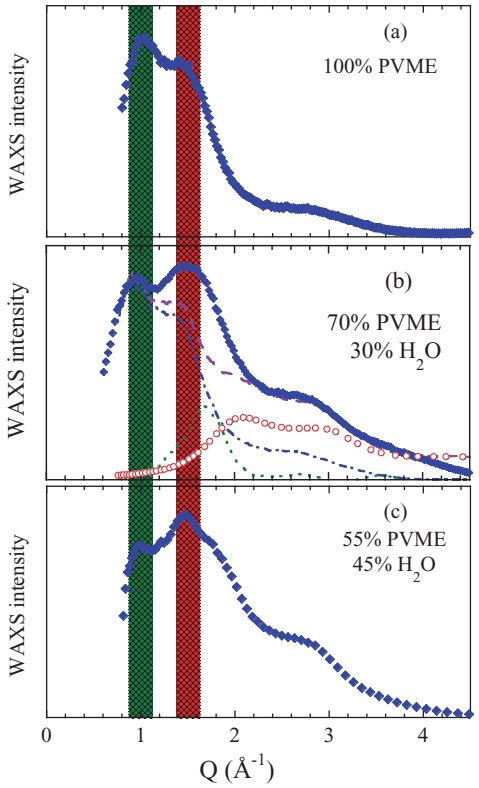

FIG. 1. (a) X-ray diffraction patterns corresponding to the dry sample, (b) a sample with 30% water content, (c) and a sample with 45% water content. The shadowed area shows the region of the first peak and the dashed area the region of the second peak. In (b), we have also plotted for comparison the patterns of the dry sample (dashed-dotted line) and of water at RT (Ref. 76). Their intensities have been chosen such that their addition (dashed line) coincides with the 30% water content pattern at low and high Q values. The difference between the experimental curve and the dashed line is the dotted line.

2. Backscattering

The backscattering measurements on the PVME/H_2O and PVME/D_2O samples were carried out by the IN16 spectrometer[25,26] at the ILL. Working with a wavelength of 6.271 Å, IN16 offers an energy resolution of nearly Gaussian shape with δE(HWHM) $\approx 0.4\mu$eV and covers a Q-range between 0.19 and 1.9 Å^{-1}. We investigated the following temperatures: 200 K, 225 K, 250 K, 270 K, 285 K, and 298 K employing measuring times of about 7 hours. The resolution function of the spectrometer was determined from the measurement of a sample at 10 K. The acquired data were corrected for detector efficiency, sample container and absorption using the standard programs available at ILL, thus finally providing the experimental scattering function. Dry PVME backscattering results were already published.[27]

D. X-rays diffraction

Diffraction experiments were performed at room temperature using a Rigaku SAXS apparatus with WAXS image plate chamber. The MicroMax-002+ X-ray Generator System is comprised of a microfocus sealed tube X-ray source module and an integrated X-ray generator unit. Using $Cu\ K_\alpha$ transition photons of wavelength $\lambda = 1.54$Å are provided. With WAXS capabilities, we measured diffraction patterns in a Q-range from ≈ 0.7 to 5 Å^{-1}. In addition to the dry and 30%-hydrated samples, we investigated a sample with 45% hydration level. The samples (transmissions about 0.4) were hold between Kapton films (transmission: 0.96) and carefully sealed. As imaging plates are used for WAXS detection, a conversion of the intensity measured in absolute units is not easy and the results are delivered in arbitrary units.

III. RESULTS AND DATA ANALYSIS

A. Structure

Figure 1(a) shows the WAXS results on dry PVME. The pattern shows two main peaks below 2 Å^{-1}: a first one centered at about 0.9 Å^{-1} and a second one located at about 1.5 Å^{-1}. With increasing water concentration [see Figs. 1(b) and 1(c)] the relative height of the two peaks varies, becoming more intense the peak at 1.5 Å^{-1}. Furthermore, an increase of the intensity could also be envisaged for the wet samples in the higher-Q region, where dry PVME shows a peak at about 2.7 Å^{-1}.

B. Calorimetry and dielectric spectroscopy

The dielectric response of PVME-aqueous solutions was previously reported in the low frequency range ($10^{-2} - 10^6\ Hz$).[23] Basically, it was found that at low temperatures it shows a broad and symmetric peak due to the reorientation of water molecules. However, we note here that such description is not satisfactory to account for the high frequency part of the spectra at very low temperatures below $\approx 150\ K$ (see Fig. 2, where only one single main symmetric relaxation process is shown by the lines). In such range it is necessary to add a high frequency ("fast") process that was not considered in the previous publication. We note that this fast process cannot be ascribed to the presence of water crystallites since (i) the DSC measurements demonstrate that the sample was free of crystallyzation[23] (ii) the relaxation times of ice are much longer than those here deduced for the fast process. Therefore, the complex part of the spectra have been fitted using two Cole-Cole (CC) functions[28] and a conductivity term

$$\epsilon^*(\omega) = \epsilon(\omega) - i\epsilon(\omega) = -i\frac{\sigma_0}{\epsilon_0\omega} + \sum_{i=1}^{2}\frac{\Delta\epsilon_i}{[1+(i\omega\tau_i)^{\alpha_i}]} \quad (1)$$

where σ_0 is the dc conductivity and ϵ_0 is the vacuum permittivity. $\Delta\epsilon_i$ is the dielectric strength, τ_i is the characteristic relaxation time and α_i gives account for the symmetric broadening of the ith process ($i = 1, 2$: "slow," "fast"). Figure 2 shows the data at $145\ K$ along with the result of the fitting procedure. The temperature dependence of the relaxation time of both processes is presented in Fig. 3 together with the derivative of the specific heat measured by calorimetry. The strong and well defined peak in the derivative curve marks the glass-transition of the PVME/H_2O system. Below

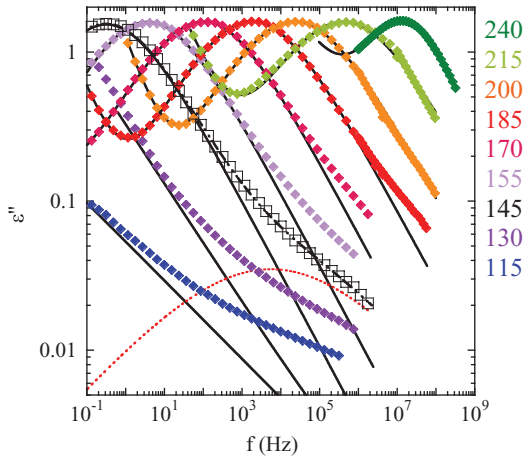

FIG. 2. Dielectric loss spectra obtained for the wet sample ($c_w = 30\%$) at the temperatures indicated (in K). The solid lines show the slow-component contribution to the spectra. For the temperature of 145 K, the fit (dashed-dotted line) containing also a fast (dotted line) contribution has been included. For temperatures above $T \approx 200$ K the "fast" process cannot be resolved.

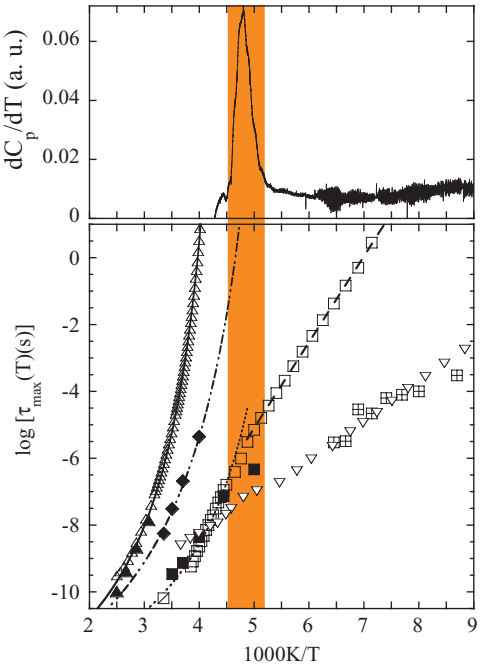

FIG. 3. (a) Derivative of the specific heat of PVME/H_2O as function of the inverse temperature. (b) Relaxation map of the PVME/H_2O system. Filled symbols: NS characteristic times at $Q = 1$Å^{-1} for the PVME (♦) and water (■) components. Empty symbols: DS relaxation times for the slow (□) and fast (⊞) processes. Results obtained on dry PVME are shown for comparison: α- (△) and β-process (▽) observed by DS, and NS characteristic times at $Q = 1$Å^{-1} (▲) (Ref. 27). The time corresponding to the maximum of the associated distribution has always been represented to compare results corresponding to different spectral shapes. Solid, dashed-dotted, and dotted lines are VF laws (see text) and the dashed line is an Arrhenius fit to the "slow" process below 200 K. Shadowed area indicates the region of the calorimetric glass-transition in the wet PVME system.

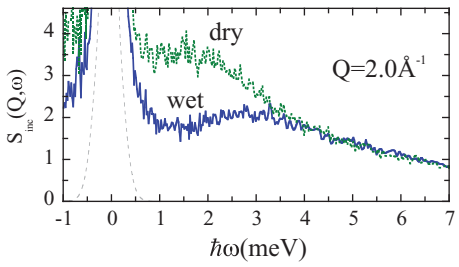

FIG. 4. Spectra obtained with FOCUS at $Q = 2.0\text{Å}^{-1}$ for dry PVME (dotted lines) and PVME/D_2O (solid lines). The dashed line shows the resolution function.

the calorimetric glass transition, the temperature dependence of the relaxation times can be described by Arrhenius equations $\tau(T) = \tau_\infty \exp(E/k_BT)$, where for a simple activated process τ_∞ corresponds to a molecular vibration time and E is the activation energy. From the fits, E results to be $0.51\,eV$ and $0.20\,eV$, with $log(\tau_\infty)$ equal to -17.8 and -12.00 for the slow and fast processes respectively. The temperature dependence of the relaxation time of the "slow" process crosses over from a non-Arrhenius dependence above T_g to an Arrhenius behavior below T_g, as observed for other water containing systems at temperatures close to T_g.[15]

C. Time of flight

Q1 The spectra in Fig. 4 show the dynamic scattering law $S(Q = 2\text{Å}^{-1}, \omega)$ for dry and wet PVME measured at FOCUS, PSI, at 100 K. In absence of relaxational processes, as it is expected at this temperature, the inelastic part of the neutron scattering spectra is determined by the H-weighted vibrational density of states (VDOS) $g(\omega)$: $S_{inel}(Q, \omega) \propto g(\omega)/\omega^2$. In glasses, the main feature of the VDOS is the so-called Boson peak of controversial origin, that manifests as a broad peak in the region around 1-5 meV. The spectra in Fig. 4 clearly reveal a Boson peak which is located for the dry PVME at about 1.5 meV and for wet PVME at a much higher energy of about 3 meV. It is evident that hydration has an impact on the microscopic dynamics of glassy PVME.

D. Backscattering

Figure 5 displays the IN16 results obtained for the PVME/D_2O sample in the supercooled liquid state. The general features are qualitatively similar to those shown by dry PVME at higher temperatures.[27] The spectra do not show an elastic component but only a quasielastic feature that broadens with increasing Q and T, suggesting diffusive-like dynamics of PVME hydrogens in the solution. We remind that the width of the spectrum is directly related with the inverse of the characteristic time of the observed process. At the same Q and T-values, the spectra recorded for the fully protonated PVME/H_2O sample are broader than those of PVME/D_2O (see as an example Fig. 6). As both contributions, that of PVME-protons and that of water-protons, are present in the PVME/H_2O spectra, it immediately follows that water motions are faster than polymer motions.

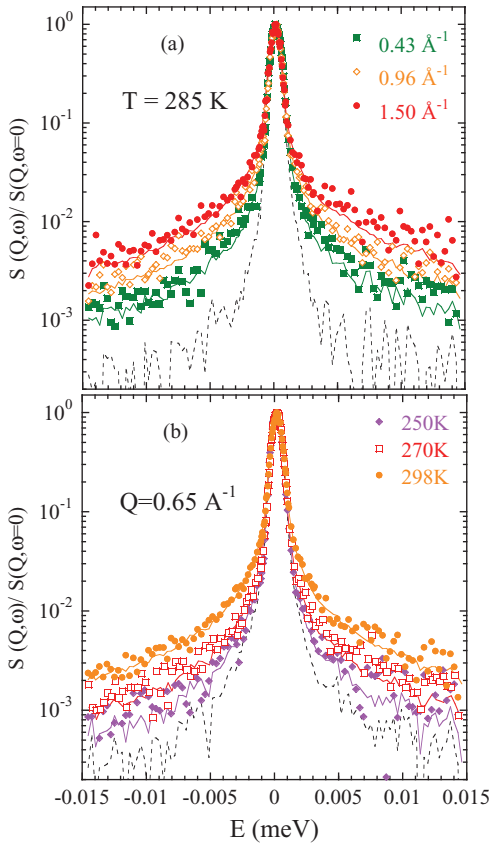

FIG. 5. Spectra obtained by IN16 on the sample where the polymer is protonated and the water is deuterated, for $T = 285$ K and three Q-values (a) and for $Q = 0.65\text{Å}^{-1}$ and three temperatures (b). The solid lines are the obtained fitting curves (Eq. (2) with $\beta^{wetPVME} = 0.3$). The instrumental resolution function is shown with the dotted lines.

In the supercooled liquid state and in the Q-region explored by BS techniques, the decay of the intermediate scattering function corresponding to atomic (H) motions of glass-forming polymers is usually phenomenologically described by a stretched exponential or Kohlrausch-Williams-Watts (KWW) functional form:

$$S_{inc}(Q, t) = A \exp\left[-\left(\frac{t}{\tau_w(Q, T)}\right)^\beta\right]. \qquad (2)$$

Here, β is the stretching parameter accounting for the deviations from exponential behavior. It can take values between 0 and 1, and for polymers is usually of the order of 0.5.[29] τ_w is the characteristic time which in general depends on both, Q and temperature. The prefactor A is an effective Lamb-Mössbauer factor that parametrizes the contribution of the fast dynamics (leading to decay of the correlation function in the ToF-window).

The IN16 PVME/D_2O results were described by Eq. (2). Given the controversy raised[30] about the fitting procedure involving FT of KWW functions that was followed in some QENS works, we mention here that in our case this function is constructed by a superposition of Lorentzian functions (FT of single exponential decays) weighted by suitable distributions of characteristic times (see Ref. 31). In this way, the problems related with the standard fitting procedure for narrow lines are avoided. In a first analysis we tried to determine the value of

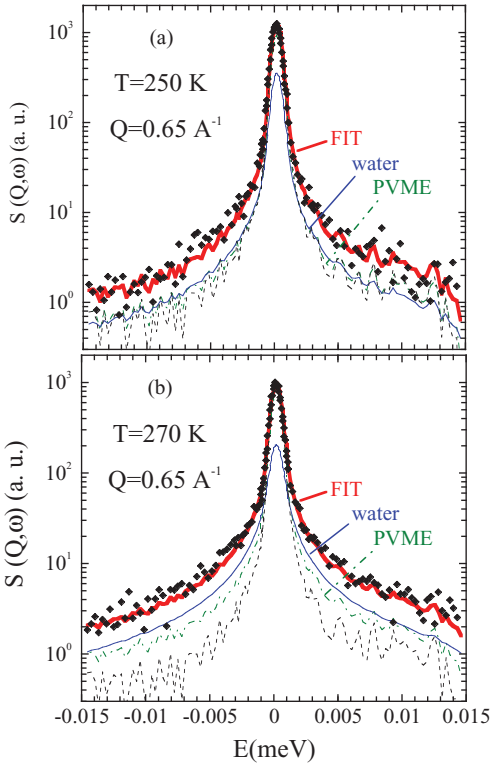

FIG. 6. Spectra obtained by IN16 on the fully protonated sample at $Q = 0.65\text{Å}^{-1}$ and two temperatures: 250 K (a) and 270 K (b). Thick solid line is the obtained fitting curve with the two contributions, from water and polymer, shown as thin solid and dashed-dotted lines, respectively. As explained in the text, the PVME contribution has been fixed according to the results obtained in the analysis of the PVME/D_2O sample. The instrumental resolution function is shown as dotted lines for comparison.

the shape parameter $\beta^{wetPVME}$ by leaving it free. Values between 0.2 and 0.4 were obtained. Fixing $\beta^{wetPVME} = 0.3$ (the average value) a good description of the spectra was achieved, as can be seen in the examples of Fig. 5. The such obtained characteristic times $\tau_w^{wetPVME}$ are shown in Fig. 7 as function of Q for different temperatures. The spectra recorded at 225 K were elastic for the IN16 resolution.

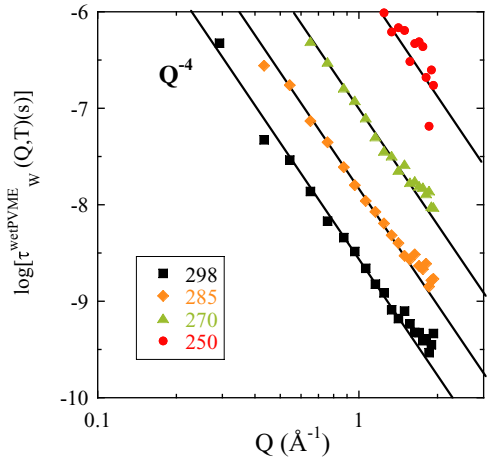

FIG. 7. Momentum transfer dependence of the characteristic times of the PVME component in the solution obtained by fixing $\beta^{PVME} = 0.3$. Solid lines show a Q^{-4}-dependence.

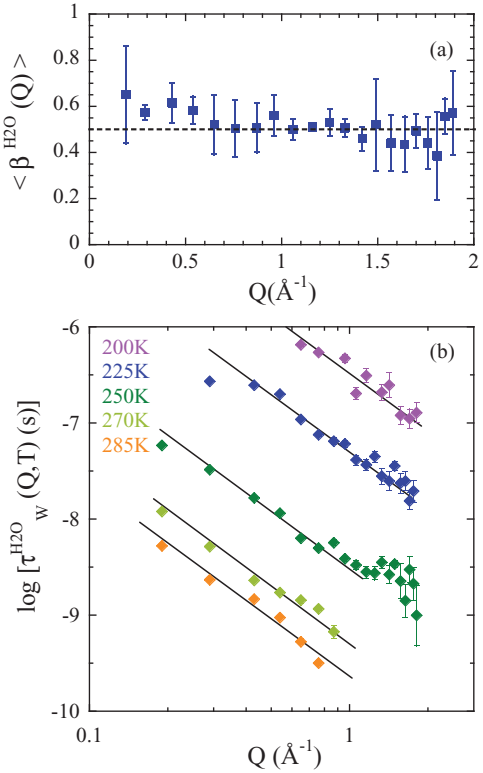

FIG. 8. Momentum transfer dependence of the T-averaged shape parameter (a) and the characteristic times (b) of the water component in the solution obtained by fixing $\beta^{PVME} = 0.3$. Dotted line in (a) marks the value $\beta = 0.5$ and solid lines in (b) show Q^{-2}-dependencies.

Information on the dynamics of the water component can be obtained from the PVME/H_2O-spectra. The total intermediate incoherent scattering function in this sample can be expressed as

$$S_{inc}^{PVME/H_2O}(Q,t) = f_{H_2O} S_{inc}^{H_2O}(Q,t) + f_{PVME} S_{inc}^{wetPVME}(Q,t) \qquad (3)$$

The weights f_{H_2O} and f_{PVME} are determined by the corresponding cross-sections: $f_{H_2O} = \sigma_{inc}^{H_2O}/\sigma_{inc}^{PVME/H_2O} = 0.31$, $f_{PVME} = \sigma_{inc}^{PVME}/\sigma_{inc}^{PVME/H_2O} = 0.69$. Taking into account the results reported for confined water dynamics in other systems,[32,33] in a first approximation the incoherent scattering function of water protons $S_{inc}^{H_2O}(Q,t)$ maybe described by a KWW function (Eq. (2)). As input for $S_{inc}^{wetPVME}(Q,t)$ we considered the results obtained from the analysis of the PVME/D_2O sample and fixed the values of the parameters in $S_{inc}^{wetPVME}(Q,t)$ to those above determined ($\beta^{wetPVME} = 0.3$, $\tau_w^{wetPVME}$ as in Fig. 7). In order to reduce the number of free parameters in the fitting procedure, we assumed that the amplitudes A parametrizing the fast dynamics of both, PVME and H_2O hydrogens, were the same. The resulting β^{H_2O}-values did not show any clear and systematic variation with temperature. The averaged values over all temperatures are shown as function of Q in Fig. 8(a), and Fig. 8(b) displays the characteristic times $\tau_w^{H_2O}$ obtained imposing the T-averaged β^{H_2O}-values in the fits.

IV. DISCUSSION

A. Structure

The interpretation of diffraction results in multicomponent systems is extremely difficult mainly due to the presence of cross-terms corresponding to correlations involving atoms of different components. The combination of results revealing different partial structure factors (e.g. X-rays and NS on samples with different deuteration labels) might help this interpretation, but without the support of (properly validated) MD-simulations the univocal assignment of the peaks to the different atomic pair correlations is practically impossible. Such a combined investigation is indeed very interesting but beyond the scope of this work. Our discussion is thus based on qualitative arguments.

The most salient effect of hydration on the WAXS patterns is the increase of the structure factor in the region corresponding to the second peak already existing in dry PVME at 1.5 Å^{-1}. This enhancement becomes more important with increasing water concentration. From simulations on the dry sample, Saelee *et al.*[34] showed that the first peak mainly contains correlations involving main-chain atoms while the second peak is predominantly due to correlations involving side-group atoms. This interpretation has been recently confirmed[35] by molecular dynamics simulation results on dry PVME properly validated with neutron scattering experiments.[27] The position of the first diffraction peak does not move upon hydration. Since this peak most probably reveals inter-chain distances between main-chain atoms, our results point to similar characteristic distances between nearest neighbor chains in the dry and the wet samples. As water can form H-bonds with the oxygen atoms in the side groups of PVME, it could be expected that the water molecules would be preferentially located close to these atoms. This hypothesis seems to be supported by the observed enhancement of the peak at 1.5 Å^{-1}. Apparently, the correlations involving water atoms emerge with the same associated characteristic lengths as the side groups in dry PVME. In this framework, inclusion of water would not disturb appreciably the short-range order of PVME. In fact, the correlations at such characteristic length scales (relating side-groups) would be even potentiated by the presence of water.

In addition to the hydrophilic oxygen atom, the side group contains a hydrophobic methyl group and together with the addition of water molecules we may thus expect some structural self-organization on the molecular scale. The question arises where the water is located, in hydrophilic or hydrophobic regions or in nano-sized bulk-like "pockets." Molecular dynamics (MD)-simulations on some hydrogel models by Tamai *et al.*[36] have shown that in a PVME cell with $c_w = 50\%$, 19% of the water molecules are in hydrophilic regions, 58% in hydrophobic regions and 23% in bulk regions. Though lower water concentrations were not investigated for the PVME hydrogels, the results in poly(vinyl alcohol) and poly(N-isopropylacrylamide) point to very small amount of bulk-like water for $c_w = 25\%$. In that work, it was also found that water-water hydrogen bonds are enhanced around hydrophobic groups, especially when they are, like in PVME, in a side group. Our results would be compatible with such scenario. The diffraction data for the 45% hydration level show a somewhat specially marked feature at $\approx 1.5\text{Å}^{-1}$. We note that in this range, the structure factor of low-density amorphous ice presents a peak.[37] In addition, we could not discard the presence of additional contributions in the wet samples at Q-values above 2 Å^{-1}. High-density amorphous ice shows a peak in this region.[37] The X-ray pattern of liquid water at RT has been included in Fig. 1(b) for comparison. The dashed line shows the simplest combination of the patterns corresponding to dry PVME and bulk-like water that best accounts for the experimental results of the 30% water content sample. The dotted line is the additional intensity in the experimental data with respect to that. This extremely simple decomposition suggests that the pattern could contain bulk-like water contributions and that the cross-terms involving PVME and water correlations would be most important close to the second peak of dry PVME. However, this is obviously not the only possible combination compatible with the experimental data and no conclusive statements can be drawn from it. The only evidence for the existence of water aggregates in this sample is the qualitatively different behavior of the water dynamics as observed by BDS (for $c_w < 30\%$ only Arrhenius-like behavior is observed, against the crossover found for 30% and above).

B. Effect on the vibrational properties of PVME in the glassy state

In the deep glassy state the Boson peak is clearly observed in both the dry and the hydrated sample, as it is shown in Fig. 4. In the hydrated one the Boson peak position is shifted from 1.5 meV (corresponding to the dry sample) to ≈3 meV and the intensity is less pronounced as well. In the higher frequency range instead, both samples show almost identical spectra, suggesting that water slightly affects the higher frequency vibrational modes of the polymer. A similar hydration-induced shift of the Boson peak has already been observed for proteins in neutron scattering experiments and molecular dynamics simulation studies.[38–42] Nakagawa *et al.* suggested that the presence of hydration water affects the protein energy landscape making it more rugged. At low temperature the protein motion is trapped in a local minimum causing the characteristic Boson peak frequency to shift to higher values.[43] On the other hand, a comparative study focused on the effects of the hydrogen bonds on the Boson peak intensity and energy has been performed on different hydrogen-bonded molecular glasses by inelastic neutron scattering measurements.[44] In that work, the authors found a general relation between the hydrogen-bond density, the Boson peak energy and the Boson peak intensity: as the number of hydrogen bonds increase, the peak intensity decreases and the peak energy increases. According to those results, the Boson peak shift in the PVME/D_2O sample with respect to the dry sample could be ascribed to the effect of the hydrogen bonds formed in presence of water. The hydrogen bonds would deform the harmonic potential at the local minima provoking the shift of the Boson peak frequency. Another possible interpretation could be the presence of a distribution of elastic constants[45] in the wet sample. Those

corresponding to the H-bonds with water would be "harder," leading to the observed shift of the Boson peak.

From the Q-dependence of the decrease of the elastic FOCUS signal we can also deduce the values of the mean squared displacements $\langle u^2 \rangle$,

$$\frac{I_{elastic}(Q,T)}{I_{elastic}(Q,T\rightarrow 0)} = \exp\left(-\frac{\langle u^2\rangle}{3}Q^2\right). \quad (4)$$

At the temperature investigated (100 K) $\langle u^2\rangle^{dryPVME} = 0.066\,\text{Å}^2$, while $\langle u^2\rangle^{wetPVME} = 0.043\,\text{Å}^2$. Thus, the amplitude of the vibrations in the glassy state appears to be slightly reduced in the presence of water. We note that from our structural results we expect some water molecules to be "attached" to the side-groups of the polymer through H-bonds. A decrease of the vibrational amplitude due to this bonding would be expected. The role of H-bond networking effect in the Boson peak frequency and the amplitude of the vibrations will be investigated in future works on PVME mixtures with other solvents that do not form H-bonds.

C. Water dynamics as revealed by neutron scattering

To describe the water component in the QENS spectra KWW functions have been used with β^{H_2O}-values close to 0.5 (Fig. 8), always smaller than 1—the value corresponding to regular and homogeneous diffusion. Similar stretching parameters have been reported for hydration water in the case of biological samples (see, e. g.[32]). At the same time, within the uncertainties, the Q-dependence of $\tau_w^{H_2O}$ follows a power-law $\tau_w^{H_2O} \propto Q^{-2}$ in the IN16 window—the behavior expected for simple diffusion. As the spectral shape is not exponential, this Q-dependence implies that the displacements of water hydrogens are not distributed according to a Gaussian function.

The observed stretching of the water signal could be attributed to a distribution of mobilities. It is well known that (at least from a mathematical point of view) stretched exponential relaxation functions can be obtained from the superposition of single exponentials:

$$\varphi(t) = \exp\left[-\left(\frac{t}{\tau_w}\right)^{\beta}\right] = \int_{-\infty}^{+\infty} g(\log\tau)\exp\left(-\frac{t}{\tau}\right)d(\log\tau) \quad (5)$$

the characteristic times of which (τ) are distributed according to given distribution functions $g(\log\tau)$. For example, Fig. 9(a) shows that proposed by Rajagopal *et al.*[31,46] giving rise to a KWW function with $\beta = 0.5$:

$$g\left[\log\left(\frac{\tau}{\tau_w}\right)\right] = ln(10)\left(\frac{\tau}{4\pi\tau_w}\right)^{\frac{1}{2}}\exp\left(-\frac{\tau}{4\tau_w}\right). \quad (6)$$

In a simple diffusion process, the characteristic time is determined by the diffusion coefficient D as $\tau = D^{-1}Q^{-2}$. A distribution of mobilities $g(\log\tau)$ can be thus originated by a distribution of diffusion coefficients and the total intermediate

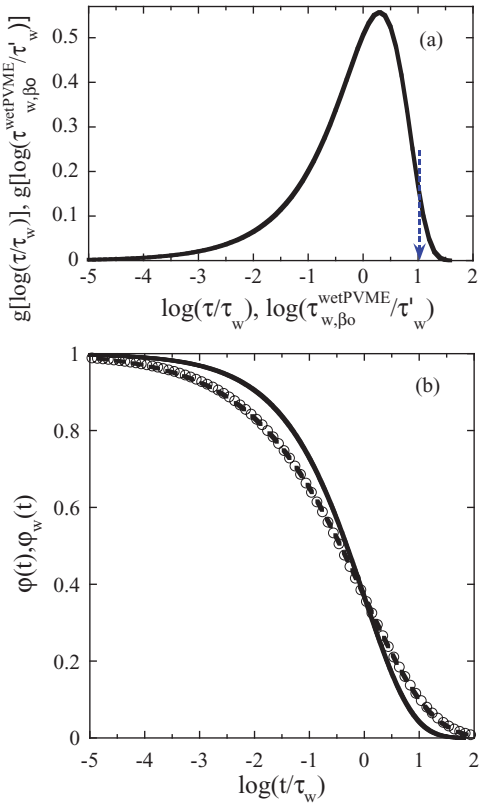

FIG. 9. (a) Distribution of characteristic times for single exponentials (Eq. (6)) and assumed to be extensible to stretched exponentials for the case of the PVME component (Eq. (11)). The superposition of single exponentials (Eq. (5)) gives rise to the KWW function with $\beta = 0.5$ shown as solid line in (b). The result of superimposing KWW functions with $\beta = 0.5$ according to Eq. (12) and characteristic times as in (a), Eq. (11), leads to the empty circles in (b) that can be described by a KWW function with $\beta = 0.36$ (dashed line). The relation between its characteristic time τ_w and the reference value of the distribution τ'_w is $\tau_w = 0.8\tau'_w$. The vertical arrow in (a) marks the corresponding value of $\tau_w^{dryPVME}$ at 298 K.

scattering function is given by

$$\varphi(t) = \exp\left[-\left(\frac{t}{\tau_w}\right)^{\beta}\right] = \int_{-\infty}^{+\infty} g(\log D^{-1})\exp\left(-\frac{Q^2t}{D^{-1}}\right)d(\log D^{-1}). \quad (7)$$

As in the case of Eq. (5), by properly choosing the distribution $g(\log D^{-1})$, a KWW time dependence of the resulting intermediate scattering function can be easily reproduced. However, now the "stretched variable" is $X = Q^2t$, i.e., the "conjugated" variable (showing the same dimension) of the distributed magnitude D^{-1}. As consequence, the resulting scattering function reads as $\exp[-(Q^2t/D_w^{-1})^{\beta}]$, which characteristic time is $\tau_w = D_w^{-1}Q^{-2}$. Therefore, the Q-dependence of the resulting characteristic time is that of each of the elementary diffusion times, $\tau \propto Q^{-2}$. Thus, we could rationalize the observed Q-dependence of the characteristic times and shape parameter of confined water assuming a distribution of mobilities or diffusion coefficients associated with slightly different local environments for the water molecules.

D. PVME dynamics in the α-relaxation regime as revealed by neutron scattering

From the BS results on the PVME/D_2O sample we can address the question how the segmental polymer dynamics is affected by the presence of water. We first summarize the results obtained for dry PVME in this Q-region well above T_g to set the reference for comparison. In a recent work that combines IN16, neutron spin echo (NSE) and FOCUS results with molecular dynamics (MD) simulations,[27] we have shown that the intermediate scattering function of PVME hydrogens can be described by a KWW function with $\beta^{dryPVME} = 0.5$. As above mentioned, this value is in the range usually found for this parameter in glass-forming homopolymers (e. g. 0.5 for head-to-head polypropylene (HHPP) and poly(ethylene propylene) (PEP),[47] 0.55 for poly(vinyl ethylene) (PVE),[48] between 0.4 and 0.65 for polybutadiene (PB),[49] between 0.4 and 0.57 for polyisoprene (PI),[50] 0.5 for poly(ethylene oxide) (PEO),[51] 0.5 for poly(methyl methacrylate) (PMMA)[52]). The characteristic times obtained for $Q = 1.0$ Å^{-1} are represented as function of temperature in Fig. 3(b). They perfectly match those obtained by DS. The coincidence of the absolute values of the characteristic times from DS and incoherent scattering at $Q = 1.0$ Å^{-1} is an empirical observation that usually holds in glass-forming polymers.[16,53] Both sets of data can be described by a Vogel-Fulcher (VF) expression:

$$\tau = \tau_\infty \exp \frac{B}{T - T_o} \tag{8}$$

with the values $\tau_\infty^{dryPVME} = 0.12$ ps, $B^{dryPVME} = 1481.5$ K and $T_o^{dryPVME} = 202$ K.

Figure 10 shows the master curve constructed scaling the characteristic times of dry PVME $\tau_w^{dryPVME}(Q, T)$ to a common reference temperature of 298 K by using Eq. (8). The good superposition obtained implies that the Q- and T-dependence of $\tau_w^{dryPVME}$ can be factorized as follows

$$\tau_w = D_{eff}^{-1}(T) f(Q) \tag{9}$$

where D_{eff} is an effective diffusion coefficient. In the region $Q \lesssim Q^\star \approx 0.7$Å^{-1}, $f(Q) \sim Q^{-x}$ with $x = 4$. We note that the exponent $x = 4$ is just equal to $2/\beta^{dryPVME}$. Inserting this Q-dependence of the characteristic time in Eq. (2), as the product $x\beta$ =2, it immediately follows that $S_{inc}(Q, t)$ is a Gaussian function with respect to the Q-variable.[54,55] In the higher-Q range above $Q^\star$ (more local scales) deviations of $\tau_w^{dryPVME}(Q, T)$ from this Q-dependence and consequently from the Gaussian approximation can be found. This kind of behavior has already been observed in a number of polymers.[47,48,50,52,56–58] These deviations can be interpreted as due to the non-Gaussian events taking place within the cage imposed by the neighboring atoms, that finally lead to the decaging involved in the structural relaxation.[57,59] Dry PVME data are consistent with the Mode Coupling Theory (MCT) phenomenological predictions.[27] Thus, the concept of caging –at the basis of this theory– plays a fundamental role in the dynamics of this polymer as observed in the BS window. As can be seen in Fig. 10, the results of dry PVME can also be well described in the framework of the anomalous jump diffusion model,[50,57] a very simple approach that incorporates the ingredient of caging by considering a distribution of jumps underlying the diffusive-like motion of protons in the α process. In this model, an atom remains in a given site for a time τ_o, where it vibrates around a center of equilibrium. After τ_o, it moves rapidly to a new position. The characteristic time follows the law

$$\tau_w = \tau_o \left(1 + \frac{1}{\ell_o^2 Q^2}\right)^{\frac{1}{\beta}} \tag{10}$$

where ℓ_o is the preferred jump distance. From the limit of this equation $\tau_w(Q \to 0) = \tau_o \ell_o^{2/\beta} Q^{-2/\beta}$ (that reproduces the expected Gaussian behavior) we may define the effective jump diffusion coefficient as $D_{eff} = \tau_o^{-1} \ell_o^{2/\beta}$, such that $\tau_w(Q \to 0) = D_{eff}^{-1} Q^{-2/\beta}$. Then $f(Q)$ in Eq. (9) can be expressed as $f(Q) = (\ell_o^2 + Q^{-2})^{1/\beta}$. For dry PVME, ℓ_o is found to be 0.65 Å (see Fig. 10). This value is larger than those obtained for main-chain hydrogens in PI (0.42 Å)[50,57] and PB (0.5 Å),[60] and close to the 0.6 Å reported for all the hydrogens in PVE.[48,60] We note that in dry PVME we are also considering both, main-chain and side-group hydrogens; therefore, the relatively large value found for ℓ_o might be a consequence of the intrinsic dynamic heterogeneity arising from different mobilities of the diverse kinds of hydrogens in the monomer. In PVE the four distinguishable kinds of hydrogens in the monomer were independently analyzed in the framework of the anomalous jump diffusion model, resulting in a distribution of values for the ℓ_o-parameter ranging from 0.32 Å for methyne main-chain hydrogens up to 0.76 Å for methylene side-group hydrogens. For dry PVME, the MD-simulations[27] show a difference in the value of ℓ_o between 0.56 Å for main-chain hydrogens and 0.75 Å for methyl-group hydrogens.

We now consider the results of PVME dynamics in the hydrated state. The obtained characteristic times for $Q = 1.0$ Å^{-1} are shown as solid diamonds in Fig. 3(b). They are clearly faster than those of dry PVME. The limited

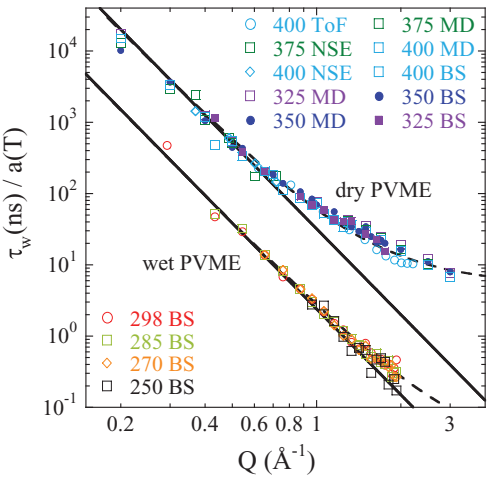

FIG. 10. Master curves obtained for dry PVME (Ref. 27) (upper curve) and PVME in the solution (lower curve) at the reference temperature of 298 K. Different symbols correspond to characteristic times obtained at the temperatures indicated in K and corrected for T-dependent shift factors $a(T)$. Solid lines show the Q^{-4}-dependence. Dashed lines correspond to descriptions with Eq. (10) with $\tau_o^{dryPVME} = 5.3$ ns, $\ell_o^{dryPVME} = 0.65$ Å, $\tau_o^{wetPVME} = 19$ ps, $\ell_o^{wetPVME} = 0.3$ Å, and $\beta = 0.5$ in both cases.

resolution of NS does not allow following the temperature dependence of these characteristic times toward the glass-transition, and the dielectric signal of PVME in the solution is masked by that of water. However, assuming that the calorimetry results [Fig. 3(a)] reflect the freezing of PVME motions in the solution (since the polymer represents the majority component in the sample) the glass-transition temperature deduced by DSC would correspond to the "effective" glass-transition of the PVME component in the solution. This implies a T_g-shift of 37 K for wet PVME arising from the presence of water –the well-know "plasticization" effect . The question arises whether the effect of water on the temperature dependence of the characteristic time of PVME can be just described by a shift in the glass-transition value (equivalently, in the Vogel temperature T_o in Eq. (8)). Under this hypothesis, i. e., assuming $T_o^{wetPVME} = 165$ K, $\tau_\infty^{wetPVME} = \tau_\infty^{dryPVME}$ and $B^{wetPVME} = B^{dryPVME}$ we obtain the dashed-dotted curve in Fig. 3(b), which perfectly describes the experimental data. It is worth noting that an analogous effect is found in polymer blends, where the vicinity of segments of chains of other kind (and displaying different intrinsic mobilities) also induces a change in the glass-transition temperature of each of the components in the mixture (see, e. g.,[61,62]).

In addition to plasticization, two other effects caused by hydration are observed in PVME dynamics: (i) a clear additional stretching ($\beta^{wetPVME} = 0.3$ vs $\beta^{dryPVME} = 0.5$) and (ii) strong deviations from Gaussian behavior in the whole Q-range investigated. Extreme stretching of the intermediate scattering function has also been reported for hydrated proteins[63] and non-Gaussian behavior has also been found in NS studies of biological samples.[64,65] In our case, the deviations from Gaussian behavior are deduced from the Q-dependence $\tau_w^{wetPVME} \propto Q^{-x}$, $x = 4$ (Figs. 7 and 10) together with the value of 0.3 for the stretching parameter. In this case, the product $x\beta$ is about 1.2, i. e., much smaller than the value of 2 corresponding to the Gaussian approximation. We remind that for the water component we have also found stretching ($\beta^{H_2O} \approx 0.5$) and deviations from Gaussian behavior ($x^{H_2O}\beta^{H_2O} \approx 1$). In Sec. IV C, these findings have been rationalized as due to a superposition of simple diffusive process originated by the existence of heterogeneous environments in the solution. The water results would be compatible with the distribution function shown in Fig. 9(a). It is natural assuming that these heterogeneous environments would produce an analogous distribution of mobilities for PVME hydrogens. We thus consider that the functional form of the PVME response in solution is KWW with a stretching parameter β_o, and the characteristic time $\tau_{w,\beta_o}^{wetPVME}$ varies from one region to the other in the sample according to the function $g(\log \tau_{w,\beta_o}^{wetPVME})$. This function would have the same functional form as that observed for the characteristic time of the water component [Eq. (6), Fig. 9(a)]:

$$g\left[\log\left(\frac{\tau_{w,\beta_o}^{wetPVME}}{\tau_w'}\right)\right] = ln(10)\left(\frac{\tau_{w,\beta_o}^{wetPVME}}{4\pi\,\tau_w'}\right)^{\frac{1}{2}} \times \exp\left(-\frac{\tau_{w,\beta_o}^{wetPVME}}{4\tau_w'}\right). \quad (11)$$

Here τ_w' is a reference timescale. The resulting response of PVME in the solution would then be given, in parallel to Eq. (5), by:

$$\varphi_w(t) = \int_{-\infty}^{+\infty} g\left(\log \tau_{w,\beta_o}^{wetPVME}\right) \times \exp\left[-\left(\frac{t}{\tau_{w,\beta_o}^{wetPVME}}\right)^{\beta_o}\right] d\left(\log \tau_{w,\beta_o}^{wetPVME}\right). \quad (12)$$

where the integral kernel is a stretched exponential function with β_o. In analogy with the case of water, where we have assumed "bulk"-like (simple diffusion) behavior for the distributed functions, for β_o we will assume a value equal to 0.5, i. e., that of dry PVME. Figure 9(b) shows with open circles the result of such superposition. This function is well described by a KWW (dashed line) with a characteristic time $\tau_w = 0.8\tau_w'$ and a value of 0.36 for the stretching parameter, i. e., very close to that used for the parametrization of the wet PVME scattering function. Thus, the stretching of both components is reproducible by assuming single-component-like functional forms and basically the same underlying distribution of mobilities,[66] i. e., invoking a common heterogeneous environment as the possible source.

So far we have shown that distributions of mobilities would explain the stretching of the PVME scattering function. The question that arises now is as follows: how does the distribution function of relaxation times that reproduces the experimental findings compare with the characteristic time in dry PVME? From the direct comparison of the master curves (Fig. 10) and the previous discussion it is clear that there is a shift in the characteristic times toward smaller values in the solution. Let us first consider the Q-range below $Q^\star$, where dry PVME shows Gaussian behavior. In this region, $\tau_w^{wetPVME}$ is just proportional to $\tau_w^{dryPVME}$ ($\tau_w^{wetPVME} = \alpha\tau_w^{dryPVME}$). The temperature dependence of α is given by the ratio between the VF equations describing wet and dry PVME results, and it takes the value of $\alpha = 0.075$ for the reference temperature of the master curves. The vertical arrow in Fig. 9(a) shows the corresponding position of the value of $\tau_w^{dryPVME}$ at this temperature, showing that $\tau_w^{dryPVME}$ is about the longest time that can be found in the solution. Most wet PVME hydrogens would move about 5 times faster than in bulk. Thus, in this Q-regime, the phenomenology observed for wet PVME could be described assuming the above scenario with reference times of the distributions like in Eq. (9), i. e., $\tau_w' = D_{eff}'^{-1}(T)f(Q)/0.8$, where $D_{eff}' = D_{eff}^{dryPVME}/\alpha$ and $f(Q)$ the same as in the dry sample. As it has been shown above, the resulting $\tau_w^{wetPVME}$ would then display the same dependence as $\tau_w^{wetPVME}$, namely Q^{-4}, according to the experimental findings (Figs. 7 and 10). We note that in the Q-range above $Q^\star$, however, this simple picture does not apply. There, $\tau_w^{wetPVME}$ shows a different Q-dependence than $\tau_w^{dryPVME}$. Nevertheless, it can still be factorized, like for dry PVME, according to Eq. (9). If we assume the validity of the scenario of superposition of KWW functions (Eqs. (12) with (11), that reproduces the stretching), then we have to admit a

different Q-dependence $f(Q)$ of the characteristic times of PVME dynamics in the solution with respect to the bulk in this high Q-range. Invoking the description of $\tau_w^{wetPVME}$ in the framework of the anomalous jump diffusion model (Eq. (10)), we could explain the results assuming that the characteristic length involved in the elementary jumps is reduced to about $\ell_o = 0.3$ Å by the presence of water (see Fig. 10). This would imply a more continuous-like diffusion of PVME atoms in the solution. We also note that for dry PVME the characteristic time at $Q^\star$ is much larger than for wet PVME, for which $Q^\star \approx 1.5 \text{Å}^{-1}$. The ratio $\tau_w^{dryPVME}(Q^\star_{dryPVME})/\tau_w^{wetPVME}(Q^\star_{wetPVME})$ is about 3 orders of magnitude, i. e., much larger than that of about 13 for the characteristic times in the Gaussian regime of dry PVME below 0.6 Å^{-1}: the decaging process would take place rather soon in the hydrated polymer.

At this point it is worth commenting that if the value of $Q^\star$ would be correlated with the location of the first structure factor peak, as suggested in some works,[16] this peak should be shifted toward higher Q-values in presence of water. Our WAXS results do not show hints of such a shift.

The above proposed is one of the simplest possible scenarios one could invoke to give account for the behavior of the polymer in presence of water. Of course, we cannot discard other possibilities or the existence of other ingredients not captured by the distribution of mobilities induced by structural heterogeneities that would also lead to deviations from Gaussian behavior at local length scales. In particular, it would be expected that the formation of a H-bond with water in the side-group would slow down the dynamics of the methyl-group with respect to the main-chain. This could give rise to an additional dynamic heterogeneity in PVME dynamics, which could translate into an additional broadening of the diffusivities (this could explain the "extra"-stretching in $\beta^{wetPVME}$ from 0.36 – see above discussion, Fig. 9 – to the observed one of 0.30). Moreover, the hindrance imposed by the H-bond would be expected to lead to smaller values of the preferred jump distance ℓ_o for the methyl-group hydrogens, leading to the resulting decrease of the value deduced for ℓ_o of all the hydrogens in our above analysis. Unfortunately, with the data at hand the dynamics of the different PVME hydrogens in the aqueous mixture cannot be selectively resolved and we cannot quantify this effect.

E. "Fast" processes observed by dielectric spectroscopy

The characteristic times of the "fast" process resolvable in the dielectric spectra at low temperatures (squares with crosses) very much coincide with those corresponding to the β-process of dry PVME (inverted triangles). This leads to think that the "fast" process in PVME/H_2O could have its origin in the motions involved in the β-relaxation of PVME. From the concentration dependence of the amplitude of the "fast" process it is deduced that water molecules also participate in this relaxation. Therefore, the "fast" process could be seen as due to the polymer localized motions involved in the β-relaxation of pure PVME and some water dynamics directly induced by the polymer motions.[67] In Ref. 67, the molecular motions corresponding to the β-process in dry PVME were assigned as the free rotational motions of the methyl ether groups around the bond connecting the oxygen and the main-chain carbon. The observation that the dynamics of water molecules reflect to some extent this kind of rotational motions would support the hypothesis that water is located close to PVME side-groups, forming H-bonds with oxygen atom and/or in the vicinity of the methyl group, as suggested by the diffraction data and found in the simulations of Ref. 36.

F. Putting the different observations into a context

In the following, we compare the results corresponding to both components (discriminated by NS) and the relaxation techniques study and put the observations into a context.

The characteristic times deduced for water from NS experiments at $Q = 1.0$ Å^{-1} are shown as solid squares in Fig. 3(b). They are much faster than those observed for the polymer component (solid diamonds), implying a strong dynamic asymmetry in the system. In an operative way, the dynamic asymmetry in a binary system Δ can be defined as the ratio between the characteristic time of the slow component and that of the fast component. This ratio increases with decreasing temperature, implying that the dynamic asymmetry in the system is enhanced when the temperature decreases. For example, at 280 K $\Delta = 100$ and at 250 K, $\Delta = 1000$. In the region $T \lesssim 225$ K, the polymer component is expected to be effectively frozen with respect to the water component and Δ assumes an effectively infinite value. Slower mobilities are also found in proteins than in the corresponding hydration water, as for example in Refs. 32, 64, 68, and 69.

In the T-range above 225 K the characteristic times of water at $Q = 1.0$ Å^{-1} overlap very well with the dielectric spectroscopy results. The empirical observation that the DS characteristic times coincide in absolute value with the incoherent scattering times at this Q-value supports the interpretation that the DS signal is reflecting the water component. The combined set of data (DS, Microwaves and NS) in this high temperature range shows that the water behavior presents some curvature indicative of cooperative-like motions. In this region, the data can be described by the VF shown in Fig. 3(b) as a dotted line, that corresponds to $\tau_\infty^{H_2O} = 0.15$ ps, $B^{H_2O} = 897$ K and $T_o^{H_2O} = 158$ K.

Below 225 K we observe that both, DS times and NS times deviate toward a weaker T-dependence. Thus, our NS results also show what has been attributed to the "strong-fragile transition" in other NS studies on water-containing systems and criticized by others.[22,30] We note that in the present case this transition occurs in the region of the overall glass-transition temperature of the sample (shaded area in the figure) which, as above commented, is mainly due to the "effective" glass-transition of the PVME majority component. Therefore, the crossover found at about 225 K can be interpreted as a signature of the onset of confinement of water by the freezing of the surrounding polymer matrix. The origin of this phenomenon should then be attributed to the strong dynamic asymmetry developed in the system at

low temperatures, in a similar way as it has been found in polymer blends (see below).[58,62,70–73]

We also note that the characteristic time obtained from NS at 200 K is faster than that deduced from the dielectric spectra at the same temperature and seems to approach the "fast" dielectric process (squares with crosses). The "fast" process in PVME/H_2O cannot be resolved above 145 K (see Fig. 2). We may assume that it can be represented by the β-relaxation of dry PVME, that can be well followed toward higher temperatures due to the higher value of its glass-transition temperature. As can be seen in Fig. 3(b), the timescale deduced from the NS experiments is close to that of the PVME secondary relaxation, but slightly slower. We could conclude that the dynamics observed by NS for water hydrogens at 200 K is a combination of both, the "slow" and the "fast" processes detected by DS, but would be mainly influenced by the "fast" process. In this framework, the source of deviations from the VF-like T-dependence of the NS results would be the occurrence of water motions strongly coupled to the PVME process involved in the β-relaxation.

As a general comment, it is worth emphasizing the analogies found between the behavior in the solution and that reported for miscible polymer blends. The phenomenology of polymer blend dynamics shows two main aspects: broadening of the responses with respect to those of the homopolymers and dynamic heterogeneity (distinguishable mobilities of the different components). As we have seen, these two features are also present in the PVME/H_2O-system. In polymer blends, the additional stretching is attributed to concentration fluctuations in the sample. In the particular case of the blend PVME / polystyrene, the additional broadening of the PVME response with respect to that of bulk PVME was described in terms of a distribution of "PVME"-like responses.[74] That situation is completely analogous to the one here presented. Moreover, under certain conditions, polymer blends can also show strong dynamic asymmetry. This happens approaching the "effective glass-transition" of the slow component in blends where the T_g-values of the homopolymers are very different. In some of such blend systems (where the slow component is also the majority component), confinement effects for the fast chains have been reported that strongly resemble those here observed for water (e. g., Arrhenius-like temperature dependence of the characteristic times in the low-T region, where the slow component is frozen[62,70]).

Finally, we note that the shift in the T_o-value of wet PVME with respect to the dry sample also implies a change in the fragility of the polymer, defined in the usual way as

$$m = \frac{d(log_{10}\tau)}{d\left(T_g/T\right)}. \qquad (13)$$

The value of m decreases from $m^{dryPVME} = 85$ to $m^{wetPVME} = 72$. In solution, the polymer becomes "stronger" in the Angell's classification. Network glass-forming systems are usually "strong" in this meaning. This observation is compatible with a relevant presence of H-bondings in the system.

V. SUMMARY AND CONCLUSIONS

The structural characterization suggests that the correlations involving water atoms emerge with the same associated characteristic lengths as the side-groups in dry PVME and that inclusion of water does not appreciably disturb the average inter-chain distances of PVME. The patterns could also be compatible with the presence of bulk-water-like correlations, that would suggest the existence of aggregates of water molecules in the sample.

By combining neutron scattering and H/D labeling, we have selectively studied the dynamics of the two components, water and polymer, in the PVME/H_2O system revealing the following:

(1) Strong impact of the presence of water on the vibrational density of states of PVME deep in the glassy state.
(2) Stretching of the scattering functions with respect to those of the components in the bulk.
(3) Non-Gaussian behavior in the whole Q-range investigated for both components.
(4) Strong dynamic asymmetry, that increases with decreasing temperature.
(5) For $T \lesssim 225$ K, deviations of the temperature dependence of the characteristic time of the water component from its high-temperature behavior.

As we have been commenting along the discussion, similar observations have been made in biological systems.[75] On the other hand, the dielectric spectra basically revealing H_2O dynamics show two main processes at low temperatures:

(6) The "fast" process can be attributed to water motions strongly coupled with the β-process of the PVME component as observed in the dry sample.
(7) At $T \approx 225$ K, the "slow" process undergoes a transition from Arrhenius-like at low temperatures to VF at high temperatures.

The comparison of dielectric spectroscopy with neutron scattering results has supported the interpretation of the dielectric data as characteristic for the water component.

To explain these results we propose:

Points (2) and (3) can be explained invoking a distribution of mobilities for both components, probably originating from structural heterogeneities present in the sample. The existence of water clusters as proposed e. g. in the MD simulations work of Tamai *et. al*[36] could be one source of such heterogeneities. In solution, PVME would move faster and in a more continuous way than in the bulk. The latter finding could be due to the formation of H-bonds with water molecules, one of the possible reasons also for Point (1). The broad distribution of mobilities found for the polymer could also be partially due to H-bond formation, that could slow down the methyl-group dynamics with respect to the main-chain dynamics. However, from our measurements we cannot resolve the dynamics of both kinds of hydrogens.

Point (5) could be due to the participation of water molecules in fast motions coupled with PVME local relaxations - the water dynamics in the NS window seems to be mainly dictated by the "fast" process (Point (6)). The

deviation expressed in Point (5) could also be interpreted as a signature of the onset of confined dynamics of water by the freezing of the PVME matrix. This would also be the origin of Point (7), which would be explained without invoking any "strong-fragile" transition. We remind that the strong slowing down of PVME motions has been directly selectively observed by the neutron scattering experiments. In this scenario, the dynamic asymmetry directly proved by the neutron scattering experiments (Point (4)) would be the key ingredient. In this context, we note that the overall phenomenology found strongly resembles that observed for polymer blends with different glass-transition temperature for the two homopolymers and where H-bonds do not necessarily exist. This similarity supports the above interpretation of some of the results in PVME/H_2O as consequence of the dynamic asymmetry in the system.

Finally, we would like to emphasize the parallelism found between the dynamical features of our "simple" system and of biological samples. This confirms that our polymer solution captures many properties observed in systems of biological nature. Therefore, without forgetting the obvious relevance of H-bond formation, we suggest that the importance of heterogeneous environments, local (secondary) relaxations of the macromolecules and dynamic asymmetry deduced here for the case of our polymer/water mixture could also be extensible to biological systems.

ACKNOWLEDGMENTS

S. C. acknowledges the grant of the "Donostia International Physics Center" (DIPC). This work is partially based on experiments performed at the Swiss spallation neutron source SINQ, Paul Scherrer Institute, Villigen, Switzerland. We thank support by the DIPC, the European Commission NoE SoftComp, Contract NMP3-CT-2004-502235, the projects MAT2007-63681, IT-436-07 (GV) and the Spanish Ministerio de Educacion y Ciencia (Grant No. CSD2006-53).

[1] F. Franks, Biophys. Chem. **96**, 117 (2002).
[2] L. Zhang, L. Wang, Y.-T. Kao, W. Qiu, Y. Yang, O. Okobiah, and D. Zhong, Proc. Natl. Acad. Sci. U.S.A. **104**, 18461 (2007).
[3] I. Brovchenko and A. Oleinikova, *Interfacial and confined water* (Elsevier, Amsterdam, 2008).
[4] S. H. Chen, L. Liu, E. Fratini, A. Faraone, and E. Mamontov, Proc. Natl. Acad. Sci. U.S.A. **103**, 9012 (2006).
[5] L. Liu, S. H. Chen, A. Faraone, C.-W. Yen, and C.-Y. Mou, Phys. Rev. Lett. **95**, 117802 (2005).
[6] J. Swenson, H. Jansson, and R. Bergman, Phys. Rev. Lett. **96**, 247802 (2006).
[7] S. Cerveny, J. Colmenero, and A.Alegría,Phys. Rev. Lett. **97**, 189802 (2006).
[8] A. Faraone, L. Liu, C.-Y. Mou, C.-W. Yen, and S.-H. Chen, J. Chem. Phys. **121**, 10843 (2004).
[9] F. Mallamace, M. Broccio, C. Corsaro, A. Faraone, U. Wanderlingh, L. Liu, C.-Y. Mou, and S.-H. Chen, Phys. Rev. Lett. **95**, 117802 (2005).
[10] S. Pawlus, S. Khodadadi, and A. P. Sokolov, Phys. Rev. Lett. **100**, 108103 (2008).
[11] C. Gainaru, A. Fillmer, and R. Böhmer, J. Phys. Chem. B **113**, 12628 (2009).
[12] K. Grzybowska, A. Grzybowska, S. Pawlus, S. Hensel-Bielowka, and M. Paluch, J. Chem. Phys. **123**, 204506 (2005).
[13] S. Capaccioli, K. L. Ngai, and N. Shinyashiki, J. Phys. Chem. B **111**, 8197 (2007).
[14] K. L. Ngai, S. Capaccioli, and N. Shinyashiki, J. Phys. Chem. B **112**, 3826 (2008).
[15] S. Cerveny, A. Alegría, and J. Colmenero, Phys. Rev. E **77**, 031803 (2008).
[16] J. Colmenero, A. Arbe, and A. Alegría, J. Non-Cryst. Solids **126**, 172–174 (1994).
[17] A. Arbe, D. Richter, J. Colmenero, and B. Farago, Phys. Rev. E **54**, 3853 (1996).
[18] D. Richter, A. Arbe, J. Colmenero, M. Monkenbusch, B. Farago, and R. Faust, Macromolecules **31**, 1133 (1998).
[19] A. Arbe, A. Moral, A. Alegría, J. Colmenero, W. Pyckhout-Hintzen, D. Richter, B. Farago, and B. Frick, J. Chem. Phys. **117**, 1336 (2002).
[20] V. García-Sakai and A. Arbe, Curr. Opin. Colloid Interface Sci. **14**, 381 (2009).
[21] H. Jansson, R. Bergman, and J. Swenson, J. Phys. Chem B **109**, 24134 (2005).
[22] M. Vogel, Phys. Rev. Lett. **101**, 225701 (2008).
[23] S. Cerveny, J. Colmenero, and A. Alegría, Macromolecules **38**, 7056 (2005).
[24] S. Capponi, "■■■," ■■■ (to be published). Q3
[25] B. Alefeld, M. Birr, and A. Heidemann, Naturwiss. **56**, 410 (1969).
[26] B. Frick and M. Gonzalez, Physica B **201**, 8 (2001).
[27] S. Capponi, A. Arbe, F. Alvarez, J. Colmenero, B. Frick, and J. P. Embs, J. Chem. Phys. **131**, 204901 (2009).
[28] R. H. Cole and K. S. Cole, J. Chem. Phys. **10**, 98 (1942).
[29] D. Richter, M. Monkenbusch, A. Arbe and J. Colmenero in "Neutron Spin Echo in Polymer Dynamics," *Advances in Polymer Science* (Springer Verlag, Berlin, 2005), Vol. 174.
[30] W. Doster, S. Busch, A. M. Gaspar, M. S. Appavou, J. Wuttke, and H. Scheer, Phys. Rev. Lett. **104**, 098101 (2010).
[31] D. Gómez and A. Alegría, J. Non-Cryst. Solids **34**, 246 (2001). Q4
[32] S.-H. Chen, L. Liu, X. Chu, Y. Zhang, E. Fratini, P. Baglioni, A. Faraone, and E. Mamontov, J. Chem. Phys. **125**, 171103 (2006).
[33] J. Swenson, H. Jansson, W. S. Howells, and S. Longeville, J. Chem. Phys. **122**, 084505 (2005).
[34] C. Saelee, T. M. Nicholson, and G. R. Davies, Macromolecules **33**, 2258 (2000).
[35] S. Capponi, Ph.D. dissertation, Universidad del País Vasco (UPV/EHU), 2011.
[36] Y. Tamai, H. Tanaka, and K. Nakanishi, Macromolecules **29**, 6750 (1996).
[37] M. M. Koza, B. Geil, H. Schober, and F. Natalia, Phys. Chem. Chem. Phys. **7**, 1423 (2005).
[38] M. Diehl, W. Doster, W. Petry, and H. Schober, Biophys. J. **73**, 2726 (1997).
[39] P. J. Steinback, R. J. Loncharich, and B. R. Brooks, Chem. Phys. **158**, 383 (1991).
[40] J. Fitter, Biophys. J. **76**, 1034 (1999).
[41] G. Caliskan, A. Kisliuk, A. M. Tsai, C. L. Soles, and A. P. Sokolov, J. Chem Phys. **118**, 4230 (2003).
[42] A. Paciaroni, A. Orecchini, S. Cinelli, G. Onori, R. E. Lechner, and J. Pieper, Chem. Phys. **292**, 397 (2003).
[43] H. Nakagawa, Y. Joti, A. Kitao, and M. Kataoka, Biophys. J. **95**, 2916 (2008).
[44] O. Yamamuro, K. Takeda, I. Tsukushi, and T. Matsuo, Physica B **311**, 84 (2002).
[45] W. Schirmacher, G. Diezemann, and C. Ganter, Phys. Rev. Lett. **81**, 136 (1998).
[46] A. K. Rajagopal and K. L. Ngai, in *Relaxations in Complex Systems*, edited by K. L. Ngai, G. B. Wright (North-Holland, Amsterdam, 1991).
[47] R. Pérez Aparicio, A. Arbe, J. Colmenero, B. Frick, L. Willner, D. Richter, and L. J. Fetters, Macromolecules **39**, 1060 (2006).
[48] A. Narros, F. Alvarez, A. Arbe, J. Colmenero, D. Richter, and B. Farago, J. Chem. Phys. **121**, 3282 (2004).
[49] A. Narros, A. Arbe, F. Alvarez, J. Colmenero, and D. Richter, J. Chem. Phys. **128**, 224905 (2008).
[50] A. Arbe, J. Colmenero, F. Alvarez, M. Monkenbusch, D. Richter, B. Farago, and B. Frick, Phys. Rev. E **67**, 051802 (2003).
[51] M. Brodeck, F. Alvarez, A. Arbe, F. Juranyi, T. Unruh, O. Holderer, J. Colmenero, and D. Richter, J. Chem. Phys. **130**, 094908 (2009).
[52] A.-C. Genix, A. Arbe, F. Alvarez, J. Colmenero, B. Farago, A. Wischnewski, and D. Richter, Macromolecules **39**, 6260 (2006).
[53] D. Richter, A. Arbe, J. Colmenero, M. Monkenbusch, B. Farago, and R. Faust, Macromolecules **31**, 1133 (1998).

[54]J. Colmenero, A. Alegría, A. Arbe, and B. Frick, Phys. Rev. Lett. **69**, 478 (1992).
[55]J. Colmenero, A. Arbe, A. Alegría, and K. L. Ngai, J. Non-Cryst. Solids **172-174**, 229 (1994).
[56]B. Farago, A. Arbe, J. Colmenero, R. Faust, U. Buchenau, and D. Richter, Phys. Rev. E **65**, 051803 (2002).
[57]A. Arbe, J. Colmenero, F. Alvarez, M. Monkenbusch, D. Richter, B. Farago, and B. Frick, Phys. Rev. Lett. **89**, 245701 (2002).
[58]M. Tyagi, A. Arbe, A. Alegría, J. Colmenero and B. Frick, Macromolecules **40**, 4568 (2007).
[59]J. Colmenero, F. Alvarez, and A. Arbe, Phys. Rev. E **65**, 041804 (2002).
[60]J. Colmenero, A. Arbe, F. Alvarez, A. Narros, D. Richter, M. Monkenbusch, B. Farago, Pramana, J. Phys. **63**, 25 (2004).
[61]T. P. Lodge and T. C.B. McLeish, Macromolecules **33**, 5278 (2000).
[62]J. Colmenero and A. Arbe, Soft Matter **3**, 1474 (2007).
[63]M. Lagi, P. Baglioni, S.-H. Chen, Phys. Rev. Lett. **103**, 108102 (2009).
[64]W. Doster and M. Settles, Biochim. Biophys. Acta **1749**, 173 (2005).
[65]W. Doster, S. Cusack, and W. Petry, Nature (London) **337**, 754 (1989).
[66]The stretching observed for the PVME component ($\beta^{wetPVME} = 0.3$) would be better reproduced by the distribution function corresponding to $\beta^{H_2O} = 0.4$. We note that such resulting stretching would also be rather well compatible with the experimental data. On the other hand, we have checked that the experimental results could also be compatible with Gaussian distributions of mobilities instead of asymmetric distributions. In such case, the distribution would have a width of about 1.2 decades.
[67]O. Urakawa, Y. Fuse, H. Hori, Q. Tran-Cong, and O. Yano, Polymer **42**, 765, (2001).
[68]K. Wood, A. Frölich, A. Paciaroni, M. Moulin, M. Härtlein, G. Zaccai, D. J. Tobias, and M. Weik, J. Am. Chem. Soc. **130**, 4586 (2008).
[69]H. Jansson, R. Bergman, and J. Swenson, J. Non-Cryst. Solids **352**, 4410 (2006).
[70]C. Lorthioir, A. Alegría, and J. Colmenero, Phys. Rev. E **68**, 031805 (2003).
[71]M. Tyagi, A. Arbe, J. Colmenero, B. Frick, and J. R. Stewart, Macromolecules **39**, 3007 (2006).
[72]A.-C. Genix, A. Arbe, S. Arrese-Igor, J. Colmenero, D. Richter, B. Farago, and P. Deen, J. Chem. Phys. **128**, 184901 (2008).
[73]A.-C. Genix, A. Arbe, F. Alvarez, J. Colmenero, L. Willner, and D. Richter, Phys. Rev. E **72**, 031808 (2005).
[74]I. Cendoya, A. Alegría, J. M. Alberdi, J. Colmenero, H. Grimm, D. Richter, and B. Frick, Macromolecules **32**, 4065 (1999).
[75]Artifacts in the NS data analysis might overestimate the deviations from VF-behavior of hydration water in some proteins, as shown in Ref. 30. However, even using the proper analysis procedure, the characteristic times of water tend to deviate from the high-temperature VF-law, as can be seen Fig. 3 of Ref. 30.
[76]G. Hura, J. M. Sorensen, R. M. Glaeser and T. Head-Gordon, J. Chem. Phys. **113**, 20 (2000).

Queries

Q1: AU: In Sec II, “Time of flight” and “Backscattering” are set as Heading3 but the same are set as Heading2 in Sec. III. Please check.
Q2: AU: In the sentence beginning “In the previous subsection,” please verify “previous subsection” refers to Sec. IVC.
Q3: AU: Please provide names of all the authors, article title, and journal name in Ref. 24.
Q4: AU: Please check Ref. 31 for content errors, or provide the DOI.